CCET JOURNAL OF SCIENCE AND ENGINEERING EDUCATION
(ISSN 2455-5061) *Vol. - 3, Page-79-92, Year-2018*

Topological Optimization of Femur Bone Prosthesis Design

Felix Paul Soju[*], Sanjay Gupta[**], Ram Krishna Rathore[***]

[*]*M.Tech Scholar, Christian College of Engineering and Technology, Chattisgarh, India,*
felixpaulsoju@gmail.com
[**]*Assistant Professor, Christian College of Engineering and Technology, Chattisgarh, India,*
sunjau02@email.com
[***] *Assistant Professor, Christian College of Engineering and Technology, Chattisgarh, India,*
krish.rathore@email.com

Abstract

With rising numbers of total hip arthroplasty (THA), optimization of orthopedic prostheses is carried out in this work to reduce the chances of implant failure or increase prosthesis consistency. This goal is achieved by first identifying the reasons for crack propagation then with the reduction of stress concentrations at the boundary between bone and implant. However, sterilerelaxing of the implant is mainly subjective to bone restoration phenomena revealed in some regions of the femur when implant is introduced. As a result, bone restoration appears due to stress shielding, that is to say the minimization of the stress level in the implanted femur caused by the significant load carrying of the prosthesis due to its higher stiffness. A maximum stiffness topological optimization-based (TO) strategy is utilized for non-linear static finite element (FE) analyses of the femur–implant assembly, with the aim of minimizing stress shielding in the femur and to furnish guidelines for re-designing hip prostheses. This is done by using an extreme accuracy for both the three-dimensional reconstruction of the femur geometry and the material properties assigned as explicit functions of the local densities.

Index Terms: *Topological optimization, Femur prosthesis, Trabecular bone tissue, Stress shielding*

1 Introduction

Every year, globally, over 800,000 total hip arthroplasty (THA) operations are done. Due to osteoporosis, rheumatoid arthritis and traumatic cases, these counts are increasing as a result of the increase of the average age of the people. Also, a large number of hip replacements in younger patients, who generally are more active and thus inflict more repeated and rigorous loads to the joint than elderly people, have been recorded in the recent years. Bad implant orientation or imprecise indexing of the prosthesis can determine aseptic mobilization phenomena that could result in catastrophic effects in the long period. After replacement surgery frequent complication may also occur, represented by a mechanical relaxing of the implant. This is characterized by implant movement and remodeling of the bone around the prosthesis, bone remodeling being the physiological dynamic response of the bone to the natural loads. The gain or loss of bone within the proximal femur when a stem is present is the main factor influencing the performance of the prosthesis and therefore its durability.

However stress shielding is one of the main factors responsible for loosening of cement less implants, radio-graphic proof based on medical follow-ups tells that surface treatments and the use of extensively porous-coated total hip arthroplasties can considerably limit the influence of stress shielding on the durability of the implant Engh et al. [1]. However, failure of osseointegration does occur in femoral amendments performed with extensively porous-coated stems Hamilton et al. [2]. However, in cemented implants, catastrophe of the femoral prosthesis component of a total hip replacement system is mainly credited to failure of the cement implant interface and cement mantle in cemented systems Beckenbaugh and Ilstrup[3]; Maloney [4]; Jasty et al. [5] and a partial role is therefore played by stress shielding phenomena Harris [6].

To avoid these types of catastrophes, possible new prosthesis profiles can be predicted by using, in common design optimization procedures, objective functions that include a measure of the stress in the cement layer surrounding the prosthesis Yoon et al. [7] or at the cement prosthesis interface Huiskes and Boeklagen[8]; Katoozian and Davy [9] with the goal of minimizing stress concentration in these areas, decreasing the likelihood of prosthesis catastrophe and maximizing prosthesis

trustworthiness. However, the choice of computational strategies based on the design optimization leads to an improved shape design of the implant stem Nicolella et al. [10]; Tanino et al. [11] and this produces two main drawbacks. The first one is related to the trouble of defining geometric compatibility between implant shape and housing femur. The second one is due to the requirement of completely modifying surgical instrumentations and consolidated techniques.

Other researchers have come up to the problem of improving the hip prostheses performance by trying to comprehend the phenomenon of loosening e.g., Rietbergen et al. [12], as well as connecting it to prosthesis design e.g., Weinans et al. [13]; Huiskes and Rietbergen[14], by means of optimization of the implant-femur response in terms of optimal bone remodeling at the interfaces. Usually, these models assume the bone-stem interface to be in contact without friction where the stem is not coated and fully bonded where coated. In reality, this is a correct approach if one considered in complete bone growth in the coated zones, and consequently, the interface bone layer supports both shear and traction without any catastrophe. However, the bone remodeling after a total hip arthroplasty is an evolutionary process, i.e., in a post-operative state, the bone ingrowth does not exist but, if the local mechanical circumstances allow, it can appear. Interface circumstances and the bone ingrowth process have been researched in several research contributions e.g., Keaveny and Bartel[15],as well as methods that incorporate ingrowth analysis and bone remodeling Fernandes et al. [16].

When the prosthesis is hosted into the femur, the new distribution of the stresses prompts bone atrophy and therefore bone restoration can appear in areas near to the implant. Indeed, due to the major overall stiffness, the prosthesis receives a significant percentage of the forces transmitted at the acetabular level and the stress in the bone minimizes with respect to its physiological magnitude, defining stress shielding Huiskes et al. [17] and then implant loosening.

Bone would absorb greater load if the stem were eliminated from the implant. This observation has led to the design of stem-less implants. However, Munting and Verhelpen [18] have claimed that stem-less implants are useful only for short-term results. In another research, hollow geometry has been introduced by increasing stem inner diameter to reduce stress shielding Gross and Abel [19], but the usage of simplified cylindrical shape, load and boundary conditions did not provide dependable quantitative approximations. Stress shielding can also be reduced if stem is made from a less stiff material which has Young's modulus equal to boneMorscher and Dick [20], but a flexible implant may produce higher stresses along the interface Huiskes,as would happen with any modulus mismatch.

However, the medical follow-up recommends that one of the critical parameter to study in a pre-clinical assessment of a new prosthetic design is the *primary stability* of cement-less hip prostheses, crucial for long-term reliability of the implant. The main features responsible for primary stability are generally accepted in the shear stresses and micro-motions happening at the interface of bone and implant. The amount of movement and the interfacial stresses depend on geometrical and mechanical properties of the prostheses. As a result, for initial stability, the accuracy of host bone preparation and the design of the prosthesis are imperative Gotze et al. [21]. Although there is no agreement in literature for the range of acceptable micro-motion at the bone–implant interface, it is seen that interface micro-motion around 40 μm gives partial ingrowth, while micro-motion exceeding 150 μm inhibits bone ingrowth completely Pettersen et al. [22]. Bone growing into porous-coated areas on the implant comprehended by means of surface treatments with hydroxyapatite or titanium plasma spray ensures osteointegration and then determines the so called *secondary stability*.

Actually, with reference to aseptic loosening of the implant, it is difficult to differentiate among the reasons inducing primary and secondary stability. A good initial fixation and then the success of a THA is indeed the result of the mixture of different interactions and simultaneouslydimensional reconstruction of the femur model and a suitable voxel size for the FE mesh were adopted. The bone material properties were varied with the local density read by means of high-resolution QCT data. Comparison between the actual stress level in the intact femur to the femur with optimized implants, as well as in various changing factors, and their collaboration gives good chances for the implant to achieve initial stability and to preserve it in the long run. [23].

Table 1 Synoptic table of the material properties assigned in relation to the density values obtained by means of QCT data

Proximal trabecular QCT level (HU)	**Isotropic Young's modulus (MPa)**	**Distal trabecular QCT level (HU)**	**Isotropic Young's modulus (MPa)**
7.825	307.03	7.825	416.14
53.731	530.13	53.731	704.43
99.637	753.23	99.637	992.72
145.54	976.34	145.54	1281
191.45	1199.4	191.45	1569.3
237.35	1422.5	237.35	1857.6
283.26	1645.6	283.26	2145.9
329.17	1868.7	329.17	2434.2
375.07	2091.8	375.07	2722.5
420.98	2315	420.98	3010.7
Proximal cortical QCT level (HU)	Isotropic Young's modulus (MPa)	Distal cortical QCT level (HU)	Isotropic Young's modulus (MPa)
>450	22000	>450	22000
Diaphysis cortical QCT level (HU)		Transversally isotropic Young's moduli	
		In-plane (MPa)	Out-plane (MPa)
>450		17700	22000

From the mechanical point of view, the factors influencing the primary stability of the stem depend on bio-mechanical interaction between femur and prosthesis. "Improper" loading of the implant after surgery can cause excessive interface shear motions and/or bone resorption, leading to implant deboning and mobilization. The term "improper" is here utilized to denote any stress level exceeding a prescribed threshold (for example, the limit shear stress at the bone–implant interface) or below a minimum stress magnitude, necessary to retain a pre-THA physiological stress level in bone and avoiding stress shielding. Then, with the objective of refining primary stability in hip prostheses, in the present study, we look at the femoral stem as a material to optimize over its volume by locally penalizing the implant stiffness through an updated mass density distribution. The map of the density distribution is achieved by means of an FE topological optimization analysis. By refining the prosthesis-bone stiffness ratio, a higher stress level is touched within the proximal and distal femur regions and, as a result, a decrease of stress shielding is obtained.

Substantial care has been given to the creation of the FE model. Faithful imitations of actual geometries of the bone and implant were created. Precise mechanical properties of the materials involved in the analysis and physiological boundary conditions were examined.

These works were made to ensure reliable qualitative and quantitative numerical results. For example, the accuracy in the three-dimensional modeling of geometry and mechanical properties of the femur was done by direct quantitative computed tomography (QCT) acquisition. This was done by considering the bone density distribution with respect to the actual levels of mineralized bone in the trabecular and cortical regions and recognizing the element size with the size of the voxels (about 1 millimeter). Each element has been assigned a corresponding elastic modulus by using the experimentally figured relations of the mechanical properties to the density and CT numbers achieved from literature for human bone Rho et al. [24]. This was done by taking into account an inhomogeneous the sub-set of elements corresponding to cancellous bone (see Table 1). A model of about 400,000 brick elements was constructed, from which an FE model of 80,000 tetrahedral elements was generated by homogenizing the local material properties over the tetrahedral element volumes.

An initially linearly elastic FE analysis of the femur, under the given loads employed by Simoes et al.[25], was

achieved to calibrate the numerical model. Simoes et al defined experiments made on a composite femur monitored with 20 uniaxial strain gauges to study the response of the bone model under physiological load conditions. We replicated the force boundary conditions applied to the femur in the experiments of Simoes et alin our numerical model. Our numerical results for displacements and strains showcased very good agreement with those attained by means of strain gauges by Simoes et al. In reality, despite the obvious differences between the materials (composite femur in the Simoes case and bone in our simulation), the application of more physiological applied boundary conditions essentially gave a reduction of bending in the bone and a more even strain distribution in some regions, as already obtained by Simoes et al. This benchmark analysis, however, has not been included in the present paper.

To exmine the possible influence of micro-motion effects at the bone–implant interface on the optimization results, contact and friction parameters have been modulated within physically reasonable ranges, as detailed in Sect. 2. However, we did not study the effects of interference fit Abdul-Kadir et al. [26], interfacial micro-motion thresholds Reggiani et al. [27,28] and remodeling phenomena Fernandes et al. on the hip stem stability.

The focus subject and the main advance of the present work are the usage of the FE topological optimization-based (TO) procedure for estimating the decreasing in stress concentration at the interfaces and the stress shielding in proximal and distal femur regions, for various percentages of implant mass reduction. The TO analysis accomplished recommend an effective penalization of the prosthesis stiffness less than proportional to the implant density distribution, without a full elimination of material. i.e., the stresses determined by the FE analysis inside the low-density implant regions were not disappearing and thus only a reduction of material stiffness should be essential. We conclude that the application of topology optimization strategies to THA design as well as to a variety of orthopedic prostheses can contribute to significantly increase performance and durability of the implants.

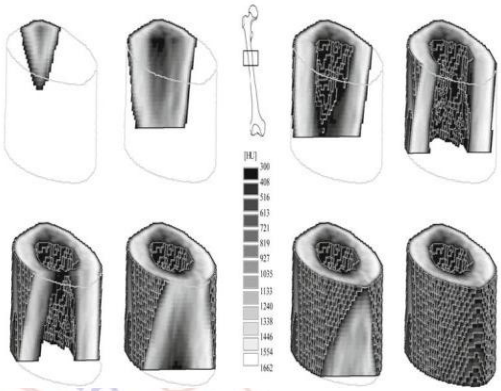

Fig. 1 The sequence of images shows the automatic 3D reconstruction of the femur diaphysis from posterior to anterior side in a sequence of*panels* starting at the *upper left*

2 Methods

2.1 Automatic generation of the prosthesis and femur models

In order to make the computational FE model, a anthropological femur was scanned by QCT. The QCT scanned the bone along 1 mm separated parallel planes and created 512 × 512 bitmap images recording the levels of material density. QCT gives density levels in terms of Hounsfield Units (HU), as a function of the X-ray attenuation into the examined material. This information, as well as the image size, is archived in DICOM standard format file. Thus, a custom-made ANSYS environment macro was developed to create FE volumes with voxel sizes, by utilizing pixel spacing, pixel thickness and image position deduced from the DICOM file and then filtering the HU for matching the actual bone range. The order of images in Fig. 1 shows the automatic 3D reconstruction of the femur diaphysis districts from posterior to anterior side.

The overall 3D model of the femur was made with the density data archived as local (voxel) information about the spatial distribution of trabecular and cortical regions.

By using the experimental literature tests made on several samples of trabecular and cortical bone tissues (Rho [29]; Rho et al., the bone density is transformed into material properties; say elastic moduli, using a custom-made algorithm able to correlate the HU in output from

QCT to corresponding mechanical parameters.

The bone cortical areas, selected by means of the HU values, are modeled as transversely isotropic, with in-plane (for example in the plane of the diaphysis cross-section) Young's modulus equal to 17,000 MPa, and the out-plane modulus equal to 22,000 MPaTurner et al. [30]. Also, we adopt isotropy for the spongy bone sites, the spatial difference of the bone density being accountable for the non-homogenous elastic response. Although, the choice of a very fine meshes in the FE-model, (see Fig. 1), ensures that structural gradients over the RVE are negligible because the RVE size is assumed to be equivalent with the FE size: this avoids clashes in terms of the relation between structural gradients and elastic symmetry Cowin[31].

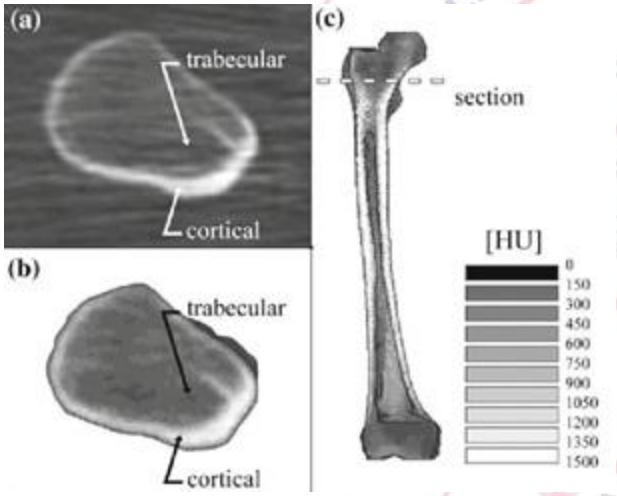

Fig. 2 The material property reconstruction process: **a** a slice of theQCT density image at the trochanteric level; **b** the corresponding sec-tion of the FE model, where it was set the *grey-scale* with reference to the material properties assigned to the different elements on the base of the local density; **c** overall frontal view section of the FE model

The assumed elastic moduli and HU levels are stated in Table 1. The accuracy of the FE model compared with QCT images, in terms of active correspondence of the X-ray density gray levels and density maps obtained by the numerical model, is shown in Fig. 2.

The automatic 3D refurbishment described above allows the operator the choice of the accuracy needed for the FE model and therefore the relation between the FE size and the number of voxels to be included into a single element. The FE shape can be taken either as a parallelepiped (*brick* elements that involve one or more voxels) or standard tetrahedral elements with quadratic shape functions defined on their sides. The final choice of the element types, as well as their mean size and possible mesh refining measures, is generally reliant on on the aim of the analysis and on the expected gradient of stress (or energy) in results. Moreover, it may be noted that the benefit of the planned automatic reconstruction method that permits one to build up a one-to-one FE model in which each voxel is recognized with a corresponding brick FE can be extremely beneficial for both performing accurate numerical simulations as well as determining the influence of the real level of mineralized bone tissue in a patient with respect to the fracture risk, this being related to the corresponding strength of the trabecular areas. A one-to-one model could still be required for the analysis of remodeling phenomena and mechanical interactions at the interface of bone and prosthesis, but one would wage the worth of a substantial computational price.

To decide the topological optimization of the implant and for the approximation of the stress shielding in the bone, tetrahedral elements are used in the ultimate analysis for mesh generation. Tetrahedral elements with refining zones are utilized where geometry and solutions in terms of stress suggest higher accuracy. This procedure, besides giving a significant computational improvement in terms of processing times and retaining a very good accuracy for the depiction of the inhomogeneous mechanical performance of the bone, has required some effort for both averaging the voxel-based density information over the corresponding element volumes and implementing CAD strategies intended to reach a suitable smooth surface of the boundary model.

The intact femur model was first created and then partitioned at the trochanteric level for inserting the implant. (The prosthesis common cement-less Ti-6Al-4V Johnson & Johnson PFC collared stem) was laser scanned and then reconstructed by a CAD system and located inside the bone. Its indexing was organized with reference to the standard surgical protocol. The elastic properties of the implant are referred to the usual literature values ANSYS Reference Guide [32]. In particular, the titanium alloy and the CrCo used for the prosthesis head and stem have been modeled as linearly elastic, isotropic and homogeneous with Young's moduli equal to 105 GPa and 210 GPa, respectively, setting 0.3 as the Poisson ratio.

The two discretized FE models are illustrated in Fig. 3 where, in order to highlight the accuracy of both the three-dimensional reconstruction and the size of the elements, a detail of the proximal region is shown.

The loads applied to both the intact and implanted femur models are shown in Fig. 4, where the joint reaction forces on the femoral head and the tractions formed by the abductors, iliopsoas and vastuslateralis muscles, are demonstrated precisely. These load circumstances are presumed to be acting statically Simoes et al. by considering multiple load scenarios to simulate different daily life activities. The numerical values of the loads, transferred to the model in terms of distributed surface loads over the concerned anatomic regions, are reported in the table associated to the Fig. 4. Also, full constraints at the base of the femur are considered.

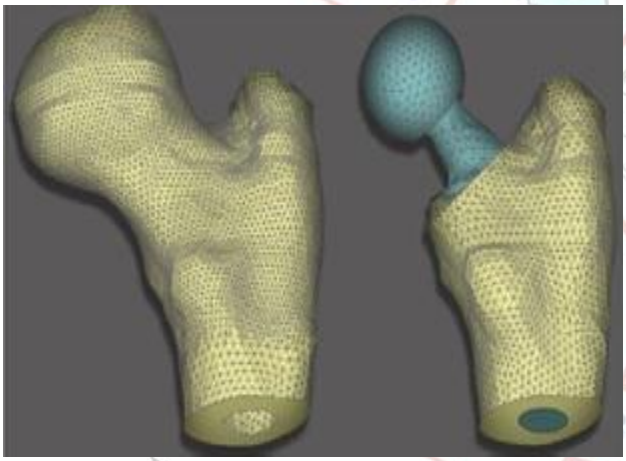

Fig. 3 The three-dimensional reconstruction of the two models.*Left*:particular of the proximal (intact) femur model and mesh; *Right*: par-ticular of the proximal femur with implant and mesh

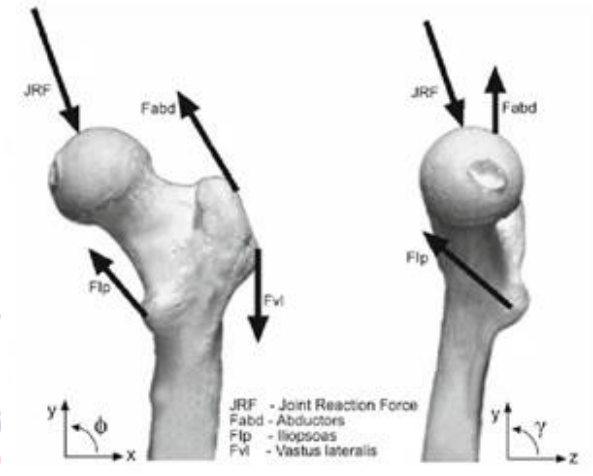

Muscle and joint reaction forces			
	resultant force	angle degree	
	(N)	ϕ	γ
joint reaction force	730	291	273
Abductors	300	110	90
Iliopsoas	188	99	137
vastus lateralis	292	270	270

Fig. 4 Load conditions applied to the femur (Simoes et al.)

Another aspect involved in the femur–prosthesis computational model is the assignment of contact with friction at the bone–implant interface. In order to simulate different situations, the values for the friction coefficient are considered variable from zero, representing only contact, to intermediate cases in which maximum 30% of perfect-bond shear stresses are relocated from the prosthesis to the femur in relation to the actual existence of compressive normal stresses Dammak[33]; Grant et al. [34]. This postulation has comported a very noteworthy increase in the computational costs in terms of time due to the combination of the non-linearity of the constraint conditions at the interfaces and the number of iterations required by the topological optimization procedure. However, no significant variations in terms of resulting optimized mass distribution of the prosthesis occurred, and very same stress distributions were listed for the contact with friction and the perfect bond cases, withreference to the specific recommended loads. Some sensitivity of the results is instead shown when a high percentage of implant mass reduction is taken. Moreover, in a recent work, Fernandes et al., with the purpose of analyzing the

remodeling processes in stem less implants, found a similar result, emphasizing the low influence of the friction coefficient on the final amount of ingrowth. However, time-depending bone remodeling phenomena Cowin and Doty [35]; Coelho et al. [36] are behind the scope of the present work.

A flow chart of the proposed numerical procedure is shown in Fig. 5.

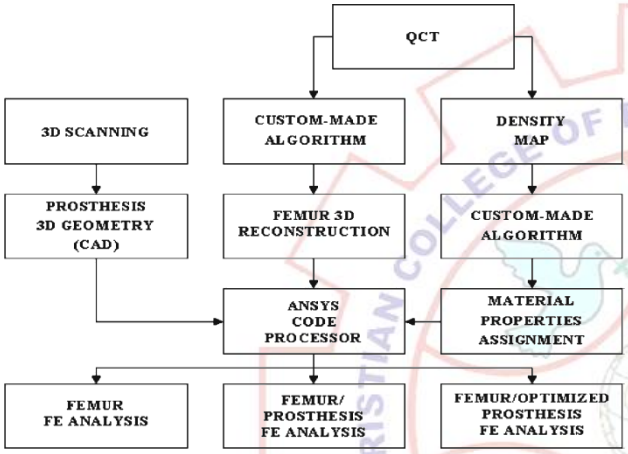

Fig. 5 Flow chart of the numerical procedure

2.2 FE implementation of the topological optimization procedure

The field of computational variable-topology shape design of continuum structures is now monopolized by methods which utilize a material distribution approach for a fixed reference domain, in the spirit of the so-called homogenization method for topology design Bendsoe and Kikucki[37]; Bendsoe and Sigmund [38]. In these models, the structure of the material is anticipated similar to a gray-scale rendering of an image, where, for example in porous media the volume fraction distribution in the solid domain establishes a continuous difference of the elastic moduli proportionately to a specific power of the ostensible density (or volume fraction). The physical goal of this supposition is usually based on the fact that transitional densities must be penalized, since the volume is proportional to the volume fraction, say ρ, but stiffness is less than proportional. Then, with reference to body forces $\boldsymbol{b}$ acting on a domain, tractions $\boldsymbol{t}$ on the boundary ∂_t and U denoting the space of kinematically permissible displacement fields, the optimal topology-shape design problem may be defined as a minimization of force times displacement, over admissible designs and displacement fields fulfilling equilibrium.

2.3 Topological optimization of the implanted prosthesis

2.3.1 Motivation

The rudimentary idea of the current study is to employ TO for establishing a appropriate mass distribution (or arrangement of voids) inside a cement less prosthesis, in order to minimize femur stress-shielding phenomena that are mainly accountable for bone resorption and thus aseptic loosening of the implant. The technique branches from a research project funded to some of the present authors since 1999 by RegioneCampa-nia, Italy (P.O.P. n°8754—Optimization of Compatible Hip Prosthesis Design), and has also fascinated the consideration of some researchers in the field, such as Ridzwan et al. [39], although with a much rougher numerical modeling and thus lacking of accurate forecasts from an engineering standpoint. Also, by considering different percentages of prosthesis volume reduction in the maximum stiffness topological optimization analysis, optimal weight and stiffness ratios are determined for dropping stress shielding in both proximal and distal regions, as well as evading stress concentrations at the bone–implant interface and inside the optimized pros-thesis.

As mentioned above, by improvising the implant/bone stiff-ness ratio, a higher stress level is reached within the proximal and distal femur areas and, as a result, a reduction of stress shielding is obtained if the topological optimization is performed over the volume originally occupied by the implant. We chose a grey-scale over a black–white optimization protocol because smooth densities admit the possibility of modeling the removal of material from the original solid domain by making micro-voids (for example, by means of micro-drilling techniques). The point being that the size of the micro-voids could be less than the mesh size (about 1-2 mm) that was taken for the numerical model. This permits the fine-tuning of the prosthesis optimization process.

Another justification that suggests the topological optimization of the prosthesis to obtain a better overall working bone–implant relationship is that maximization of stiffnessby means of reduction of the strain energy copies

the biomechanical process, regulated by growth and bone remodeling, in which the bone tissue is invited to reach its optimum configuration, e.g., remodeling equilibrium Cowin and Hegedus[40]; Cowin[41,42]; Cai et al. [43]; Jang and Kim [44,45]; Jang et al. [46]. In this optimization process, the mass distribution of the prosthesis is rearranged; thus, the implant would appear to be following its individual "Wolff's law."

Note that, by conserving the integrity of the outer shape of the implant, the optimized prosthesis does not need any modification in the production processes, implanting instrumentation and consolidated surgical procedures. Also, all the surface treatments developed for the femoral stems to promote bone ingrowth and then osteointegration could still be saved without any conflict with the features needed for the topological optimized implant Luo et al. [47]; Fernandes et al.

2.3.2 Non-linear FE analyses

Three major FE analyses have been done. The first was with respect to the intact femur. This scenario is researched both for validating the accuracy of the model and for achieving outcomes to use as benchmarks for establishing variations in terms of stress distributions in comparison with other analyses where the prosthesis is hosted in the femur.

The second study case, named "0", is the one in which the THA is simulated. This is a static analysis done for the femur with the implant; this is done for two cases, the case of a perfect bond and the case of contact with friction interface conditions. The results of these cases are used for approximating stress concentrations and stress shielding in bone in a usual THA situation and are done in the absence of an optimization procedure. This is discussed in detail below.

The last case treats the topological optimization (maximum stiffness with volume reduction constraints) of the implant, by looking into four different optimization cases, that is the case "1", where only the interior of the implant is optimized (e.g., the elements are opened onto the boundary of both the prosthetic head and the stem s their original mass), the case "2", in which the interior of the stem is optimized and the implant head is fully optimized, the case "3", representing the circumstance where the stem is fully optimized, while the only interior of the head is optimized, and finally, the case "4", in which the whole prosthesis is optimized. Also, in order to examine a sufficiently wide range of potential mass arrangements inside the optimized implants, for each cases, the optimized distribution of mass inside the femoral stem model is achieved by applying four different mass reduction percentages, that is, 55, 65, 75 and 85%. The lower (55%) and upper (85%) selected percentages of volume reduction employed in the topological optimization analysis represents a good approximation. The percentages whose respective prosthesis volume fractions are 45 and 15%, respectively, if homogeneously distributed over the implant domain, would give the comparable (upper) cortical and (lower) cancellous bone overall stiffness, respectively. These values give a required wide and physically judicious range of possible prosthesis mass reduction. This result is at par with one of the objectives of this work, namely to lessen the variation between bone and implant stiffness. This outcome may be validated with mathematical ease if the topological optimization routine is used with a power law penalization power equal to three to relate Young's modulus to the volume fraction.

3 Results

The initial analysis was done on the intact femur. The outcomes in terms of stresses propose a good accuracy of the numerical model and therefore the effectiveness of employing both a faithful three-dimensional reconstruction of the femur and the elastic non-homogeneity obtained by interpreting the density map into corresponding material properties. We note that the vector plot of the principal stresses looks like the trabecular organization in the real femur. Also, the amount of the stresses never reaches the compressive and tensile yield stresses determined locally by the bone density. Moreover, the outcomes achieved in our study show that the application of more real life boundary conditions to the femur model leads to a decreased bending in the bone and to a better uniform strain distribution, in set-up with the results exposed in experimental, strain gauged, femoral tests by Simoes et al. Thus, due to this consensus and to the accuracy of the numerical model, the outcomes stated above have been employed as reference values (for example in terms of von Mises stresses) for estimating abnormalities from the physiological stress distribution in the cases where the prosthesis is introduced, for the circumstances where the implant is optimized and when it is not.

The second FE analysis was performed on the femur with an implant, common cement less titanium alloy collared straight stem. This examination considered both perfect bond and contact with friction conditions at the interface bone–prosthesis. Several non-linear static analyses were done in order to study the conceivable influence of friction on the outcomes. As we mentioned above, friction was considered variable within the range (0-0.3). However, no significant stress variations were registered between the perfect bond and the contact with friction cases, excluding very low friction values (≈ 0). The outcomes exhibit some characteristic femoral regions where stress shielding actually produces resorption, consistent with those regions exposed by X-rays of post-surgery implantation cases. To be specific, part of the great trochanter and some distal cortical areas of the diaphysis show a significant low of the von Mises stress, in contrast with the same stress measure read on the equivalent elements of the intact femur.

Indeed, to approximate the consequence of the prosthesis on the stress distribution in the bone, the von Mises stress, designed at the centroid of each part, was selected as the base line. Broadly speaking, von Mises stress could be not precisely the most appropriate method of mechanical stimulus in anisotropic, non-homogeneous materials such as cancellous bone and thus we should not assume that resorption rest on on it. However, this is a comparatively easier, scalar measure of a stress at a point. Moreover, a study by Terrier et al. [48] approves that bone adaption models using strain energy density and the von Mises criterion give very similar outcomes.

Referring to the FE analysis where (maximum stiff-ness) topological optimization of the implant is evaluated, for different percentages in mass reduction (55, 65, 75, 85%) and for various positioning of the material mass to be optimized (cases “1”, “2”, “3” and “4”), the results were collected and presented as follows. The variation in stress for each element before and after THA was considered and divided by the stress happening in the element pre-THA to determine a “Stress Shielding Increase”, (SSI), for that area. The before and after proportions were then volume averaged over a specific region to calculate SSI for that area. Since the von Mises stress is strictly non-negative, positive stress difference values show decline in the stress level in post-THA condition, thus, stress shielding is the averages of the stresses over the designated volume elements *e*.

Disappearing SSI means disappearing stress shielding and directs an optimal condition. On the contrast, negative values of the SSI represent a rise of stress when the prosthesis is present and therefore they can be taken as a measure of Stress concentrations, specially, if the actual stress in the bone is more than yield strength or physiological based thresholds

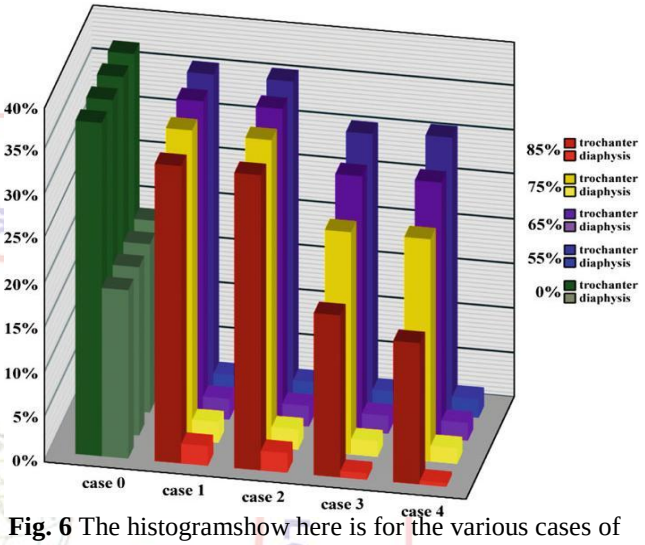

Fig. 6 The histogramshow here is for the various cases of reduction of stress shielding, calculated as a ratio between the variation of von Mises stress in the intact and implanted femur and von Mises stress within the intact femur.all magnitudes being averaged over the element volumes consistent to the trochanter and diaphysis model districts.

The Fig. 6 shows the benefit of embracing optimized prostheses. Rise of stress shielding (SSI), measured as a proportion between the variance of von Mises stress in the intact and implanted femur and von Mises stress in the intact femur, all magnitudes being averaged over the element volumes consistent to the trochanter and diaphysis model regions, and are denoted. It can be seen that, in contrast with the case “0” where the prosthesis is not optimized, the mean decrease in stress shielding is rises with the effective mass reduction percentage of the implant and the gain in reduction of stress shielding reaches about 85% (SSI of 15%) for the great trochanter, and up to 99% (SSI less than 1%) for the diaphysis.

An assessment of the stress shielding results for two cases, one in which the prosthesis maintains its initial mass and one after the optimization process, is illustrated in Fig. 7. Figure 7 comprises of four polar diagrams showing a ratio of the von Mises stresses in the two cases; these ratios are

assessed over a ring of elements placed at the trochanter level, around the implant, where usually stress shielding phenomena appear. In particular, the polar figures show the outcomes of the topological optimization in terms of a ratio between the difference of von Mises stress placed at the trochanter level (around the prosthesis) and von Mises stress in the same elements of the femur with non-optimized implant, and von Mises stress of the femur with non-optimized implant. This approximation varies from the SSI measure as it is calculated at the centroid of each designated element (no overall average on the whole set of elements), comparing the stress shielding in the case where the prosthesis is not optimized (standard case "0") with the results for optimized implants at various prosthesis mass reduction percentages. It is beneficial to note that the results reveal that the von Mises stresses in the femur with optimized implant are 90% greater than the corresponding ones in the femur with non-optimized pros-thesis. However, these values are always smaller than the von Mises stresses in the intact femur in the areas where the same stress is examined and, thus, the stress Eigen values in the intact femur are less than the compressive and tensile yield stresses.

Finally, Figs. 8 and 9 encapsulate the outcomes of the topological optimization in terms of resulting densities (RD) over the prosthesis domain and von Mises stresses (VMS) in a frontal section of the femur. There, the development of the stresses and the decrease in stress shielding with the increase of prosthesis mass reduction percentage is emphasized, as shown in the sequences of the images.

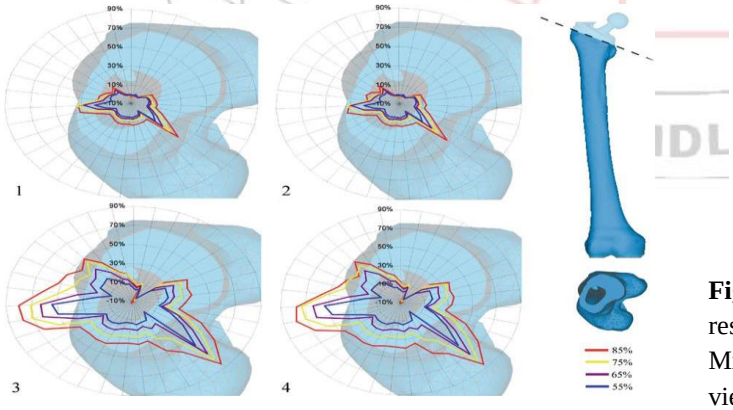

Fig. 7 Polar diagrams illustrate the outcomes of the topological optimizationin terms of a ratio between the difference of von Mises stress placed at the trochanter level (around the prosthesis) and von Mises stress in the same elements of the femur with non-optimized implant, and von Mises stress of the femur with non-optimized implant.

To stress the effectiveness of the huge number of cases scrutinized, it is valuable to note that, in traditional problems of topological optimization, the regions that display low density as a result of the optimization process are taken as material to be removed. On the contrary, in the case of optimized pros-theses, to achieve this in general, is not always possible. Indeed, if low densities appear at the interface with the bone (for example, in the cases "2", "3" and "4"), to remove material means to remove geometrical continuity and therefore loosening would be insignificant to forecast. Thus, low output densities should be taken as an opportunity of reducing stiffness, not as a necessity. From this point of view, unconventional for TO, one should then aim to design prostheses where low densities obtained as TO results recommend where to reduce material stiffness, for example, by decreasing the volume fraction using laser micro-drilling of the implant or by defining prostheses in composite materials.

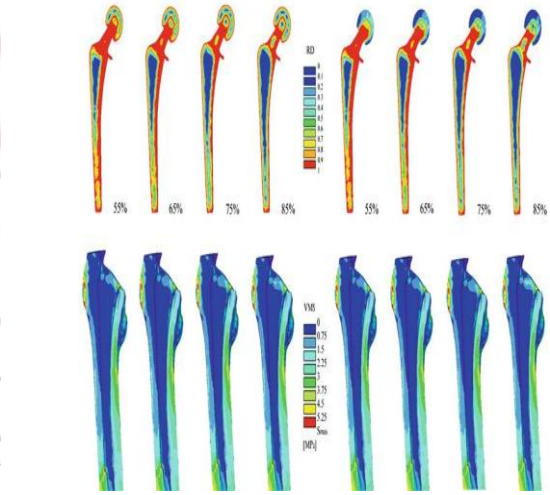

Fig. 8 Results of the topological optimization in terms of resultingdensities (RD) over the prosthesis domain and von Mises stresses (VMS) of the femur (as sectioned frontal view projections).

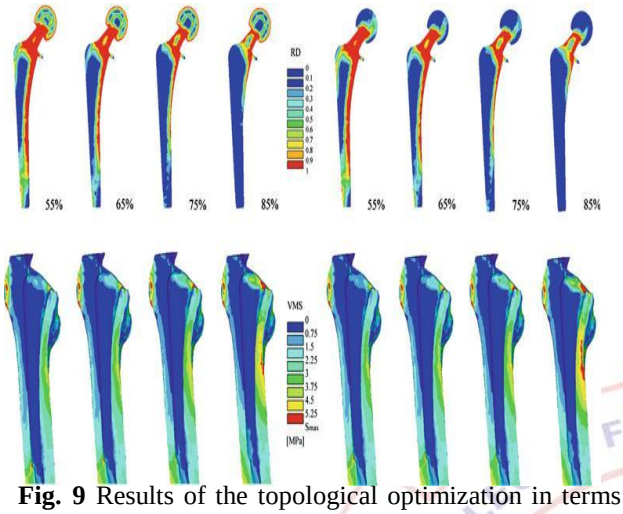

Fig. 9 Results of the topological optimization in terms of resultingdensities (RD) over the prosthesis domain and von Mises stresses (VMS) of the femur (as sectioned frontal view projections).

4 Discussion

The aim of the research done was to find possible strategies for redesigning hip prosthetics. Maximum stiffness topological optimization approaches were used to study aseptic loosening of THA implants intensely subjective by bone resorption due to stress shielding. Stress shielding is revealed in X-ray post-operative controls within the great trochanter and inside distal femur regions. In order to investigate the sensibility of the prosthesis density distribution with respect to the stress shielding increases, a large range of cases was studied, by taking into account different percentages of implant mass reduction. Good accuracy in the three-dimensional reconstruction of the femur model and an appropriate voxel size for the FE mesh were implemented. The bone material properties were varied with the local density read by means of high-resolution QCT data. Comparison between the actual stress level in the intact femur to the femur with optimized implants, as well as estimates of the stress shielding reduction in the standard and optimized prosthesis, was executed. Selecting the von Mises stress as the measure of these variations, the outcomes achieved appeared to approve that TO might be a good method for establishing THA design criteria for reducing stress shielding and thus aseptic loosening.

As we mentioned above, removal of material inside the original prosthesis is not the only engineering clarification of the implant density distribution in output from the topological optimization analyses. We observed that, in line with the spirit of TO, to preserve continuity at the interface without changing the external shape of the implant, the use of various bio-compatible materials (titanium and polymers) or laser drilling techniques for generating micro-porosity could be desirable to holed prostheses to re-design them.

It is imperative to note that, also for high mass reduction percentages, the stress state in the prosthesis never extents more than about 30% of the titanium yield strength, avoiding the likelihood to fear the influence of fatigue phenomena in the stem, at least in short-time estimates.

Finally, the major outcomes of the research can be abridged by means of the following two points:

1. The concluding map of deceptive densities acquired within the prosthesis field as a result of the TO analyses can be used as recommendation for establishing where to remove material in the re-design of the implant. In particular, one would obtain: (a) a prosthesis with optimized (maximum) ratio strength/weight, according to the physiological response of the bone; (b) a reduced distance between overall bone and prosthesis ratios stiffness/weights, with the effect of a better dynamic behavior (less alterations in proper frequencies between bone and implant); (c) a reduced stress shielding, with the effect of an accumulation of the durability of the implant due to the decrease of the aseptic loosening.

2. From the point of view of the producer, once the optimized prosthesis overcomes mechanical testing, several benefits could be envisaged: (a) the material can be taken away from the real prosthesis by means, for example micro-drilling techniques, so making void sizes that, copies the trabecular bone tissue also at the interface bone–implant, could be made in order to fuel bone in-growth, too; (b) the process of micro-drilling (or any other weakening procedure) can be made-up as an operation to do after the manufacture of a first integer stem, so evading further prices that would originate from an essential changes of the production cycle; (c) in terms of marketing, the fact that the instruments and therefore the combined surgery

practices presently embraced by surgeons do not change, would include a further advantage for the company.

However, stress shielding phenomena are not the sole mechanisms creating aseptic loosening. For example, wear debris particles, superiority of the bone–implant interface and time dependent reaction in terms of remodeling of the bone tissue and in-growth procedures are important mechanisms that have not been ventured in this research. Specially, for the aim of decreasing implant aseptic mobilization, interface dynamic processes may play a major part in the optimization.
Therefore, FEM-based topology optimization *custommade* procedures, able to straight away take into consideration both temporaryobjective functions for minimizing stress shielding and added detailed constraints, would pave the way toward new remarkable perceptions.

References

[1] Engh CA Jr, Young's AM, Engh CA Sr, Hopper RH Jr (2003) Clini-cal consequences of stress shielding after porous-coated total hip arthroplasty. ClinOrthopRelat Res 417:157–163

[2] Hamilton WG, McAuley JP, Tabaraee E, Engh A (2008) The outcome of revision of an extensively porous-coated stem with another extensively porous-coated stem. J Arthroplasty 23:170–174

[3] Beckenbaugh RD, Ilstrup DM (1978) Total hip arthroplasty. J Bone andJoint Surg Am 60:306–313

[4] Maloney WJ, Schmalzried T, Harris WH (2002) Analysis of long-term cemented total hip arthroplasty retrievals. ClinOrthop Related Res 405:70–78

[5] Jasty M, Maloney WJ, Bragdon CR, O'Connor DO, Haire T, Harris WH (1991) The initiation of failure in cemented femoral compo-nents of hip arthroplasties. J Bone Joint Surg British 73:551–558 Joshi MG, Advani SG, Miller F, Santare MH (2000) Analysis of a fem-oral hip prosthesis designed to reduce stress shielding. J Biomech33:1655–1662

[6] Harris WH (1992) Will stress shielding limit the longevity of cemented femoral components of total hip replacement? ClinOrthopRelat Res 274:120–123

[7] Yoon YS, Jang GH, Kim YY (1989) Shape optimal design of the stem of a cemented hip prosthesis to minimize stress concentration in the cement layer. J Biomech 22:1279–1284

[8] Huiskes R, Boeklagen R (1989) Mathematical shape optimization of hip prosthesis design. J Biomech 22:793–804

[9] Katoozian H, Davy DT (2000) Effects of loading conditions and objec-tive function on three-dimensional shape optimization of femoral components of hip endoprostheses. Med EngPhys 22:243–251

[10] Nicolella DP, Thacker BH, Katoozian H, Davy DT (2006) The effect of three-dimensional shape optimization on the probabi-listic response of a cemented femoral hip prosthesis. J Biomech 39:1265–1278. (opology to reduce stress shielding problem. J App Sci 6:2768–2773)

[11] Tanino H, Ito H, Higa M, Omizu N, Nishimura I, Matsuda K, Mitamura Y, Matsuno T (2006) Three-dimensional computer-aided design based design sensitivity analysis and shape optimization of the stem using adaptive p-method. J Biomech 39:1948–1953

[12] Rietbergen B, Huiskes R, Weinans H, Sumner DR, Turner TM, Galante JO (1993) The mechanism of bone remodeling and resorp-tion around press-fitted THA stems. J Biomech 26(4/5):369–382 Simoes JA, Vaz MA, Blatcher S, Taylor M (2000) Influence of head constraint and muscle forces on the strain distribution within theintact femur. Med EngPhys 22:453–459

[13] Weinans H, Huiskes R, Grootenboer HJ (1992) The behavior of adap-tive bone-remodeling simulation models. J Biomech 25:1425– 1441

[14] Huiskes R, Rietbergen B (1995) Preclinical testing of total hip stems, the effects of coating placement. ClinOrthop Related Res 319: 64–76

[15] Keaveny TM, Bartel DL (1995) Mechanical consequences of bone ingrowth in a hip prosthesis inserted without cement. J Bone Joint Surg 77(6):911–923

[16] Fernandes PR, Folgado J, Jacobs C, Pellegrini V (2002) A contact model with ingrowth control for bone remodeling around cement-less stems. J Biomech 35:167–176

[17] Huiskes HWJ, Weinans H, Van Rietbergen B (1992) The relationship between stress shielding and bone resorption around total hip stems and effects of flexible materials. ClinOrthop 274:124–134

[18] Munting E, Verhelpen M (1995) Fixation and effect on bone strain pat-tern of a stemless hip prosthesis. J Biomech 28:949–961

[19] Gross S, Abel EW (2001) A finite element analysis of hollow stemmed hip prostheses as a means of reducing stress shielding of the femur. J Biomech 34:995–1003

[20] Morscher EW, Dick W (1983) Cement less fixation of isoelastic hip endoprostheses manufactured from plastic materials. ClinOrthop 176:77–87

[21]Gotze C, Steens W, Vieth V, Poremba C, Claes L, Steinbeck J (2002) Primary stability in cementless femoral stems: custom-made versus conventional femoral prosthesis. ClinBiomech 17:267–273

[22] Pettersen SH, Wik TS, Skallerud B (2009) Subject specific finite ele-ment analysis of implant stability for a femoral stem. ClinBiomech 24:480–487

[23] Monti L, Cristofolini L, Viceconti M (1999) Methods for quantitative analysis of the primary stability in uncemented hip prostheses. Artif Organs 23(9):851–859

[24] Rho JY, Hobatho MC, Ashman RB (1995) Relations of mechanical properties to density and CT numbers in human bone. Med EngPhys 17:347–355

[25] Simon U, Augat P, Ignatius A, Claes L (2003) Influence of the stiffness of bone defect implants on the mechanical conditions at the inter-face—a finite element analysis with contact. J Biomech 36:1079– 1086

[26] Abdul-Kadir MR, Hansen U, Klabunde R, Lucas D, Amis A (2008) Finite element modelling of primary hip stem stability: the effect of interference fit. J Biomech 41:587–594

[27] Reggiani B, Cristofolini L, Varini E, Viceconti M (2007) Predicting the subject-specific primary stability of cementless implants during pre-operative planning: preliminary validation of subject-specific finite-element models. J Biomech 40:2252–2258

[28] Reggiani B, Cristofolini L, Taddei F, Viceconti M. (2008) Sensitivity of the primary stability of a cementless hip stem to its position and orientation. Artif Organs 32:555–560

[29] Rho JY (1991) Mechanical properties of human cortical and cancellous bone. Ph.D. Thesis, University of Texas Southwestern Medical Center at Dallas

[30] Turner CH, Rho J, Takano Y, Tsui TY, Pharr GM (1999) Theelas-tic properties of trabecular and cortical bone tissues are similar: results from two microscopic measurement techniques. J Biomech 32:437–441

[31] Cowin SC (2002) Elastic symmetry restrictions from structural gradients. In Rational continua: classical and new—a collection of papers dedicated to Gianfranco Capriz on the occasion of his 75th birthday, Springer, Berlin

[32] ANSYS Inc (2007) ANSYS 11 user's documentation. Canonsburg, PA

[33] Dammak M, Shirazi-Adl A, Zukor DJ (1997) Analysis of cementless implants using interface non-linear friction-experimental and finite element studies. J Biomech 30:121–129

[34] Grant JA, Bishop NE, Gotzen N, Sprecher C, Honl M, Morlock MM (2007) Artificial composite bone as a model of human trabecular bone: the implant-bone interface. J Biomech 40:1158–1164

[35] Cowin SC, Doty SB (2007) Tissue mechanics. Springer, Berlin

[36] Coelho PG, Fernandes PR, Rodrigues HC, Cardoso JB, Guedes JM (2009) Numerical modeling of bone tissue adaption—a hierarchi-cal approach for bone apparent density and trabecular structure. J Biomech 42:830–837

[37] Bendsoe MP, Kikucki N (1988) Generating optimal topologies in struc-tural design using a homogenization method. Comp Methods App MechEng 71:197–224

[38] Bendsoe MP, Sigmund O (1999) Material interpolation schemes in topology optimization. Archive App Mech 69:635–654

[39] Ridzwan MIZ, Shuib S, Hassan AY, Shokri AA, Ibrahim MNM (2006) Optimization in implant topology to

reduce stress shielding problem. J App Sci 6:2768–2773

[40] Cowin SC, Hegedus DH (1976) Bone remodeling I: theory of adaptive

[41] Cowin SC (1994) Optimization of the strain energy density in linear anisotropic elasticity. J Elasticity 34:45–68

[42]Cowin SC (1999) Bone poroelasticity. J Biomech 32:218–238
elasticity. J Elasticity 6:313–326

[43] Cai K, Chen BS, Zhang HW, Shi J (2008) Stiffness design of contin-uum structures by a bionics topology optimization method. J App Mech ASME 75:0510061–05100611

[44] Jang IG, Kim IY (2008) Computational study of Wolff's law with tra-becular architecture in the human proximal femur using topology optimization. J Biomech 41:2353–2361

[45] Jang IG, Kim IY (2009) Computational simulation of trabecular adap-tion progress in human proximal femur during growth. J Biomeh 42:573–580

[46] Jang IG, Kim IY, Kwak BM (2009) Analogy of strain energy density based bone-remodeling algorithm and structural topology optimi-zation. J BiomehEng Trans ASME 131:0110121-7

[47] Luo G, Sadegh AM, Alexander H, Jaffe W, Scott D, Cowin SC (1999) The effect of surface roughness on the stress adaption of trabecular architecture around a cylindrical implant. J Biomech 32:275–284

[48] Terrier A, Rakotamanana RL, Ramaniraka AN, Leyvraz PF (1997) Adaption models of anisotropic bone. Comp Methods Bio-mech Biomed Eng 1:47–59